RSC Advances

Cytotoxicity of fluorographene

Journal:	*RSC Advances*
Manuscript ID	RA-ART-10-2015-022663.R1
Article Type:	Paper
Date Submitted by the Author:	29-Nov-2015
Complete List of Authors:	Teo, Wei Zhe; Nanyang Technological University, Chemistry and Biological Chemistry Sofer, Zdenek; Institute of Chemical Technology, Prague, Department of Inorganic Chemistry Sembera, Filip; Institute of Organic Chemistry and Biochemistry AS CR, v.v.i., Janousek, Zbynek; Institute of Organic Chemistry and Biochemistry, Pumera, Martin; Nanyang Technological University, Chemistry and Biological Chemistry
Subject area & keyword:	Nanomaterials - Materials < Materials

Journal Name

ARTICLE

Cytotoxicity of fluorographene

Wei Zhe Teo,[a] Zdenek Sofer[b], Filip Šembera[c], Zbyněk Janoušek[c] and Martin Pumera*[a]

Received 00th January 20xx,
Accepted 00th January 20xx

DOI: 10.1039/x0xx00000x

www.rsc.org/

Fluorinated graphene (F-G) are gaining popularity in recent years and should they be introduced commercially in the future, these nanomaterials will inevitably be released into the environment through disposal or wearing of the products. In view of this, we attempted to investigate the cytotoxicity of three F-G nanomaterials in this study, with the use of two well-establish cell viability assays, to find out their impact on mammalian cells and how their physiochemical properties might affect the extent of their cytotoxicity. Cell viability measurements on A549 cells following 24 h exposure to the F-G revealed that F-G does impart dose-dependent toxicological effects on the cells, and the level of cytotoxicity induced by the nanomaterials differed vastly. It was suggested that the fluorine content, in particular the types of fluorine-containing group present in the nanomaterial played significant roles in affecting its cytotoxicity. In addition, control experiments which were conducted for possible nanomaterial-induced artifacts on the cell viability assays showed that absorbance readouts from the cell viability assays are free from interference from the nanomaterials.

Introduction

Over the past few decades, numerous studies were conducted on carbonaceous nanomaterials (nanocarbons), such as fullerenes, carbon quantum dots, nanotubes, nanofibers, nanoparticles and graphene, to investigate their physiochemical properties and applicability in various fields.[1-3] The nanocarbons were found to possess remarkable properties and are already incorporated in many commercial products. According to the latest statistics collated by The Project on Emerging Nanotechnologies (PEN) in Oct 2013, carbon is the third most frequently mentioned nanomaterial in the product descriptions of 1628 nanotechnology-based consumer products available in the market.[4] Of these nanocarbons, graphene and its family of derivatives like graphene oxide, nitrogen-doped graphene and halogenated graphene are probably the class of carbon nanomaterials that attracted the most attention among researchers in recent years due to their interesting physiochemical properties.[5-9] For instance, graphene nanomaterials functionalized with fluorine (fluorinated graphene, F-G) were reported to exhibit varying band-gap energies with different degree of fluorination and some of them displayed prominent photoluminescence in the blue/ultraviolet region, thereby allowing these nanomaterials to find potential applications in band gap engineering or optoelectronics.[10-13] The F-G nanomaterials were also determined to possess high thermal stability and the chemical inertness of fully fluorinated graphene (C_1F_1) was discovered to be comparable to Teflon.[14,15] Consequently, these nanomaterials will be expected to remain persistently in the environment when F-G are introduced commercially and consumers products containing this compound are disposed of subsequently. This situation could be detrimental to our health if these nanomaterials are toxic, hence it is crucial to examine the toxicity of F-G before they are even incorporated into future consumer devices.

Many of the studies found in the literature involving F-G focused mainly on the synthetic methods and physiochemical properties of their synthesized nanomaterials; few discussed on their toxicity. In one such study, it was demonstrated that F-G could be utilized to enhance cell adhesion and proliferation of bone marrow derived mesenchymal stem cells, indirectly proving that their F-G films were non-toxic.[16] On the other hand, another group showed that F-G sheets were able to induce toxic effects on human nerve cells (SH-SY5Y).[17] Even though information on F-G nanomaterials' toxicity are very limited, toxicity of other fluorocarbon-based organic compounds are readily available.[18,19] These organofluorine compounds exhibit varying degree of toxicity, with fluoroacetate being highly toxic to mammals and insects while fluoro-substituted alkanes and alkenes inducing little to no acute inhalation toxicity.[20-22] On top of that, fluorinated graphene oxide was found to be harmless to human breast cancer cell (MCF-7), as the nanomaterial did not show any cytotoxicity up to a concentration of 576 μg mL^{-1} fluorinated graphene oxide incubated (for 3 days).[23] It had also been suggested that the toxicity of fluorinated organic compounds are likely to be linked to their molecular characteristics.[24] In addition, we demonstrated in our recent study that cytotoxicity of fluorinated nanocarbons towards mammalian

[a] Division of Chemistry & Biological Chemistry, School of Physical and Mathematical Sciences, Nanyang Technological University, 21 Nanyang Link, Singapore 637371, Singapore. E-mail: pumera@ntu.edu.sg
[b] Institute of Chemical Technology, Department of Inorganic Chemistry, Technická 5, 166 28 Prague 6, Czech Republic
[c] Institute of Organic Chemistry and Biochemistry AS CR, v.v.i., Flemingovo nam. 2., 166 10 Prague 6, Czech Republic.

cells could be affected by the physiochemical properties of the nanomaterials.[25] The objective of this work, therefore, is to conduct similar examinations on three different F-G in order to elucidate how the differences in their physiochemical properties affect the nanomaterials' cytotoxicity towards human lung carcinoma cells (A549). The extent of toxicological effects induced by the F-G was investigated by cell viability measurements of the A549 cell line after 24 h exposure to the F-G and this cell line was preferentially chosen as the lungs are usually the first point of contact with the nanomaterials when the latter are inhaled into the body. Two well-established cell viability assays: methylthiazolyldiphenyl-tetrazolium bromide (MTT) assay and water-soluble tetrazolium salt (WST-8) assays, which produce coloured formazan dyes in the presence of viable cells, are used for this study to calculate the percentage cell viability of the A549 cells.[26,27]

Experimental

Chemicals and apparatus

Methylthiazolydiphenyl-tetrazolium bromide (MTT) assay were purchased from Sigma-Aldrich, water-soluble tetrazolium salt (WST-8) from Dojindo, and dimethyl sulfoxide (DMSO) from Tedia. High purity microcrystalline graphite (2-15 µm, 99.9995%) was obtained from Alfa Aesar, Germany. Sulfuric acid (98 wt.%), nitric acid (68 wt.%), potassium chlorate (>99%). hydrochloric acid (37%), were obtained from Penta (Czech Republic). Fluorine (20 vol.% in N_2) was obtained from Solvay, Belgium. Hydrogen (99.9999%) and nitrogen (99.9999%) were obtained from SIAD (Czech Republic).

Synthesis of fluorinated graphene

GO synthesis. The graphite oxide prepared by the Hofmann method was termed 'HO-GO'.[28] Concentrated sulfuric acid (87.5 mL) and nitric acid (27 mL) were added to a reaction flask containing a magnetic stir bar. The mixture was then cooled at 0 °C, and graphite (5 g) was added. The mixture was vigorously stirred to avoid agglomeration and to obtain a homogeneous dispersion. While keeping the reaction flask at 0 °C, potassium chlorate (55 g) was slowly added to the mixture in order to avoid a sudden increase in temperature and the consequent formation of explosive chlorine dioxide gas. Upon the complete dissolution of the potassium chlorate, the reaction flask was then loosely capped to allow the escape of the evolved gas and the mixture was continuously vigorously stirred for 96 h at room temperature before being poured into deionized water (3 L) and decanted. The graphite oxide was first redispersed in HCl (5%) solutions to remove sulphate ions and then repeatedly centrifuged and redispersed in deionized water until all chloride and sulphate ions were removed. The graphite oxide slurry was then dried in a vacuum oven at 50 °C for 48 h before use.

Microwave assisted exfoliation in hydrogenation plasma.[29] Further, 1 g of HO-GO was placed in quartz glass microwave reactor. The reactor was repeatedly evacuated and purged with high purity nitrogen. The exfoliation was performed using 2.45 GHz/1 kW power for 3 minutes under hydrogen atmosphere (50 mL min^{-1}) at reduced pressure (10 mbar). During the exfoliation, a nitrogen plasma was formed which further accelerated the exfoliation and reduction of graphite oxide. The reduced graphite oxide was further used for fluorination.

Fluorination procedure. The fluorination was performed in Teflon lined Monel autoclave using a nitrogen-fluorine mixture (20 vol.% F_2) from a dedicated fluorine line.[30] An amount of 1 g of graphene or graphite oxide was placed in the Teflon liner, the autoclave was evacuated and filled with N_2/F_2 mixture under 3 bar pressure. Various times and temperatures of fluorination were applied to investigate influence of different starting material (graphene and graphene oxide) as well as different reaction times. F-G595 was prepared by direct fluorination of graphene oxide at 180 °C for 4 days. F-G596 and F-G597 were prepared by direct fluorination of graphene synthesized by microwave exfoliation in hydrogen plasma. F-G596 was treated for 24 hours while F-G597 was treated for 4 days.

Characterisation of fluorinated graphene

Scanning electron microscopy (SEM) was performed with JEOL-7600F semi-in-lens FE-SEM in gentle-beam mode at a working distance of 5.8 – 8.5 mm, and an accelerating voltage of 0.5 – 2 kV. Combustible elemental analysis (CHN-O) was performed with a PE 2400 Series II CHN/O Analyzer (Perkin Elmer, USA). In CHN operating mode (the most robust and interference free mode), the instrument employs a classical combustion principle to convert the sample elements to simple gases (CO_2, H_2O and N_2). The PE 2400 analyzer performs automatically combustion and reduction, homogenization of product gases, separation and detection. A microbalance MX5 (Mettler Toledo) was used for precise weighing of samples (1.5 - 2.5 mg per single sample analysis). The accuracy of CHN determination is better than 0.30% abs. Internal calibration is performed using N-fenyl urea. For the measurement of fluorine concentration, the samples were decomposed for analysis according to Schöniger method. The exact amount of sample (about 2 mg) was wrapped in an ash free paper, burned in pure oxygen atmosphere and leached out with deionized water and total ionic strength adjustment buffer (TISAB) was added subsequently. The concentration of fluorine was determined by potentiometric measurement with an ion-selective electrode (ISE). XPS wide-survey and high-resolution C1s and F1s spectra measurements were performed using a Phoibos 100 spectrometer and a monochromatic Mg X-ray radiation source (SPECS, Germany) at 12.5 kV. X-ray diffraction was performed with a Bruker D8 diffractometer in Bragg–Brentano parafocusing geometry using CuKα radiation. Diffraction patterns were collected for 2θ values from 5° to 80°. The FT-IR spectra were measured using an iS50R FT-IR spectrometer (Thermo Scientific, USA). The measurement was performed using diamond ATR crystal and KBr beamsplitter.

Cell culture preparation and incubation with fluorinated graphene

Human lung carcinoma epithelial cells (A549; Bio-REV Singapore) were cultured in complete cell culture medium prepared with Dulbecco's Modified Eagle Medium (DMEM; Gibco) supplemented with 10% fetal bovine serum (FBS; PAA Laboratories), and 1% penicillin-streptomycin liquid (Capricorn Scientific GmbH). The A549 cells (cell density = 8.8 x 10^4 cells mL^{-1}) were seeded and incubated in 24-well plates at 37 °C and 5% CO_2 for 24 h and subsequently rinsed with 1x PBS before introducing fluorinated graphene suspensions (3.125 mg mL^{-1} – 400 mg mL^{-1}) for further incubation at 37 °C and 5% CO_2 for another 24 h. The control A549 cells were cultured under the same manner but were not exposed to the fluorinated suspensions.

Cytotoxicity measurements

MTT assay. A549 cells which were incubated 24 h with fluorinated graphene in 24-well plates were subjected to washing with 1x PBS for two times after removing the fluorinated graphene suspensions. Then, MTT reagent (1 mg mL^{-1}) was added to the cells and incubated at 37 °C and 5% CO_2 for 3 h. Subsequently, the MTT reagent was removed from the 24-well plates and replaced with dimethyl sulfoxide (DMSO) to dissolve the insoluble purple formazan crystals produced by the viable A549 cells. The assay liquid was transferred into individual Eppendorf tubes after gently agitating the plates for 5 mins and centrifuged (8000 rpm) for 10 mins. Lastly, the supernatant was transferred to a 96-well plate to measure its absorbance at 570 nm (and background absorbance at 690 nm). Absorbance data collected are represented relative to the absorbance of the control A549 cells (not exposed to fluorinated graphene).

WST-8 assay. A549 cells which were incubated 24 h with fluorinated graphene in 24-well plates were subjected to washing with 1x PBS for two times after removing the fluorinated graphene suspensions. Then, WST-8 reagent (10x diluted) was added to the cells and incubated at 37 °C and 5% CO_2 for 1 h. Subsequently, the assay liquid was transferred into individual Eppendorf tubes and centrifuged (8000 rpm) for 10 mins. Lastly, the supernatant was transferred to a 96-well plate to measure its absorbance at 450 nm (and background absorbance at 800 nm). Absorbance data collected are represented relative to the absorbance of the control A549 cells (not exposed to fluorinated graphene).

F-G nanomaterials-induced interference on cell viability assays

MTT assay. Fluorinated graphene-induced interference on MTT assay measurements can arise from 1) reactions between the fluorinated graphene and the MTT reagent or 2) binding of the insoluble MTT formazan product to the fluorinated graphene nanomaterials.

To examine for artifacts caused by reactions between fluorinated graphene and the MTT reagent, varying concentrations of the nanomaterial were first mixed with the MTT reagent (1 mg mL^{-1}) under cell-free conditions and incubated in 24-well plates at 37 °C for 3 h. Subsequently, the mixtures were removed and replaced with DMSO, and the 24-well plates were gently agitated for 5 mins. The assay liquids were then transferred into individual Eppendorf tubes for centrifugation (8000 rpm; 10 mins) and the supernatants obtained were subjected to absorbance measurement at 570 nm and 690 nm (background absorbance).

To examine for binding of the insoluble MTT formazan product to fluorinated graphene nanomaterials, the 3 h incubated MTT-fluorinated graphene mixtures obtained from the abovementioned experiment were mixed with ascorbic acid (4 mM) by gently agitating for 5 mins and incubated at 37 °C for 1 h so as to allow MTT reduction to take place in the absence of cells. Following incubation, DMSO was added to the MTT-F-G-ascorbic acid mixtures and placed in the incubator at 37 °C for an additional 10 mins before transferring them into individual Eppendorf tubes for centrifugation (8000 rpm; 10 mins). Lastly, the supernatants were subjected to absorbance measurement at 570 nm and 690 nm (background absorbance). The data gathered in both tests are represented relative to the control experiment (not exposed to fluorinated graphene) that was conducted under the same conditions.

WST-8 assay. The only possible fluorinated graphene-induced artifact on WST-8 assay should be caused by reactions between the fluorinated graphene and the WST-8 reagent, due to the fact that WST-8 assay produces soluble formazan product. Therefore, varying concentrations of CXF were mixed with the WST-8 stock solution to obtain resulting mixtures consisting of 10% v/v of the working WST-8 reagent, which were incubated at 37 °C for 1 h under cell-free conditions. Subsequently, the mixtures were transferred into individual Eppendorf tubes for centrifugation (8000 rpm; 10 mins) and the supernatants obtained were subjected to absorbance measurement at 450 nm and 800 nm (background absorbance). The data gathered are represented relative to the control experiment (not exposed to fluorinated graphene) that was conducted under the same conditions.

Results and discussion

Characterisation

Characterisation of the three F-G nanomaterials were performed by various analytical techniques to examine the physiochemical properties of the nanomaterials. Scanning electron microscopy (SEM) was carried out to determine the morphology of the F-G nanomaterials. Elemental composition was investigated with a combination of combustible elemental analysis (CHN-O) and ion-selective electrode (ISE) measurement for fluorine concentration determination. Furthermore, X-ray photoelectron spectroscopy (XPS) was performed to investigate the types of carbon bonding present in the nanomaterials. The structure and chemical composition was investigated using X-ray diffraction and infrared FT-IR spectroscopy with Furrier transformation (FT-IR). The information obtained from the characterisation of the F-G nanomaterials will enable us to better interpret and understand the cytotoxicity data collected from the cell

viability measurements as physiochemical properties of a nanomaterial are the primary factors that affect its toxicity.[31,32] SEM images of the three F-G nanomaterials (Figure SI-1) revealed that the degree of exfoliation of F-G595 and F-G597 is much higher than that of F-G595. This is in agreement to the synthesis procedure of the three F-G nanomaterials, where F-G595 was prepared directly from the fluorination of graphene oxide while in the synthesis of F-G596 and F-G597, the graphene oxide were microwave exfoliated first before the fluorination procedure. Also, increasing amounts of charging were observed from F-G595 to F-G597, which could be due to the nanomaterials becoming more insulated as more fluorine atoms are present in the nanomaterial.

Table 1. Atomic percentage (at.%) of elements present in the F-G nanomaterials. All values (except for fluorine) are acquired from combustible elemental analysis (CHN-O). Values for fluorine are derived from ion-selective electrode (ISE) measurements.

Material	Carbon, C	Hydrogen, H	Nitrogen, N	Oxygen, O	Fluorine, F
F-G595	74.6	8.1	0.0	15.7	1.5
F-G596	46.7	7.3	0.1	3.2	42.6
F-G597	36.4	2.8	4.9	5.2	50.7

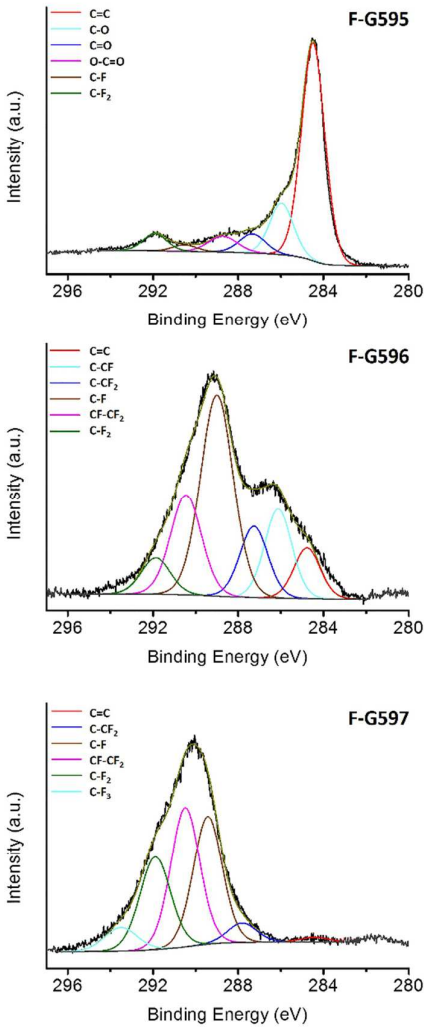

Figure 1. High resolution core-level C 1s X-ray photoelectron spectra (XPS) of the three F-G nanomaterials, F-G595, F-G596 and F-G597.

Table 1 summarizes the atomic percentages (at.%) of all elements found in the three F-G nanomaterials. From the values, it was clear that both F-G596 and F-G597 nanomaterials were highly fluorinated, with as much as 50.7 at.% F found in F-G597. F-G595, on the other hand, can be described as fluorine-doped graphene nanomaterial as only 1.5 at% of F is present in the nanomaterial. Further analysis of the F-G nanomaterials' chemical composition through deconvolution of their high-resolution core-level C 1s X-ray photoelectron spectra (Figure 1) revealed that all three nanomaterials contain C=C (284.5 eV) C-F (289.0 eV) and C-F_2 (291.9 eV) bond types in different amounts. In addition, other carbon-fluorine bond types were found in F-G596 and F-G597, namely C-CF (286.1 eV; F-G596 only), C-CF_2 (287.3 eV), CF-CF_2 (290.5 eV), and C-F_3 (293.5 eV; F-G597 only).[33,34] Besides fluorine-containing groups, oxygen-containing groups such as epoxy/hydroxyl (C-O; 286.0 eV), carbonyls (C=O; 287.3 eV), and carboxylic acids (O-C=O; 288.7 eV) were detected in F-

G595 which contained at least thrice the at% of oxygen as compared to F-G596 and F-G597. As graphene are functionalized with increasing number of fluorine atoms (from F-G595 to F-G597), the planar structure becomes increasingly puckered as the carbon atoms change from sp^2 to sp^3 hybridization. Consequently, the fluorinated graphene will adopt different structural arrangements like chair, stirrup, boat or twist conformations, and it has been reported that while the chair configuration is the most stable conformer for fully fluorinated graphene, the stirrup configuration played a significant role in a mixed fluorinated graphene sample.[35,36] Therefore, F-G596 and F-G597 are likely to possess the chair conformation, whereas F-G595 is expected to adopt the stirrup configuration.

The structural properties were further investigated by X-ray diffraction. The significant increase of interlayer spacing and broadening of reflections can be seen with increasing of fluorine content. The interlayer spacing increased from 0.369 nm for F-G595 on 0.706 nm and 0.719 nm for F-G596 and F-G597, respectively. The results of X-ray diffraction are shown on Figure Si-2.

The FT-IR spectroscopy measurement gives more information's about the chemical bonds in fluorinated graphene. The FT-IR spectra of F-G596 and F-G597 spectra are dominated by C-F vibration band located around 1150 cm^{-1}. The C-F band is significantly weaker in sample F-G595 with lower concentration of fluorine. The results of FT-IR spectroscopy are shown on Figure SI-3.

With a better knowledge on the elemental content and types of carbon bonds available in these three F-G nanomaterials, we would be able to establish the relationship between these features and the nanomaterials' cytotoxicity, if any.

Cytotoxicity measurements

We examined the toxicological effects of F-G on A549 cells through the use of two cell viability assays, namely methylthiazolyldiphenyl-tetrazolium bromide (MTT) assay and water-soluble tetrazolium salt (WST-8) assays. Both MTT and WST-8 assays contain active viability markers which will be reduced in the presence of viable cells, generating coloured formazan in the process.[26,27] The colour intensity of the final assay will then reflect the amount of metabolically active cells available in the cell culture, and by calculating the relative absorbance of the F-G-incubated A549 cell culture to the control A549 cell culture (not exposed to F-G), the cytotoxicity of the F-G can hence be deduced. With the use of two cell viability assays that function on similar principles, the reliability of the data collected would be ensured unless opposing trends are obtained.

Absorbance readouts of the MTT assay after incubating with A549 cells (F-G exposed) were acquired and shown as percentage cell viability in Figure 2. It can be observed from the figure that all three F-G induced dose-dependent cytotoxicity on the A549 cells, as a trend of decreasing A549 cell viability with increasing dosage of F-G introduced can be seen across all three nanomaterials tested. This dose-dependent toxicological effect is especially evident for F-G596, where the percentage cell viability changed from 95.8% at the lowest concentration of 3.125 μg mL^{-1} to 22.5% at the highest concentration of 400 μg mL^{-1} F-G596 exposure. At the highest concentration of F-G exposure, cell viability of the A549 cells incubated with F-G595, F-G596 and F-G597 were 76.8%, 22.5% and 73.0% respectively. Hence, based on the MTT assay assessment, the order of the level of cytotoxicity exhibited by the three F-G is F-G596 > F-G597 > F-G595; F-G596 is the most toxic while F-G595 is the least toxic.

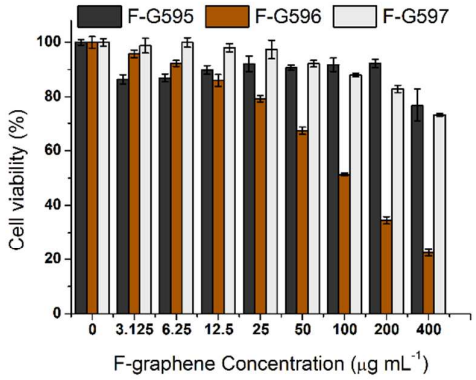

Figure 2. Percentage cell viability of A549 cells that were incubated with varying concentrations of F-G nanomaterials for 24 h. The percentages are derived from MTT assay absorbance measurements and are relative to the absorbance values from A549 control cells that were not treated with F-G nanomaterials. Data represent mean ± standard deviation.

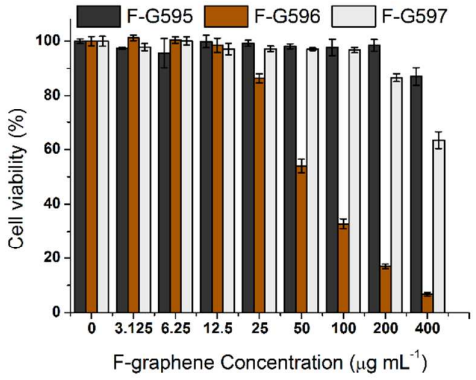

Figure 3. Percentage cell viability of A549 cells that were exposed to varying concentrations of F-G nanomaterials for 24 h. The percentages are derived from WST-8 assay absorbance measurements and are relative to the absorbance values from A549 control cells that were not treated with F-G nanomaterials. Data represent mean ± standard deviation.

Figure 3 displays the percentage cell viability derived from A549 cells (F-G exposed) which were incubated with WST-8 assay. Unlike MTT assay, the active viability marker 2-(2-methoxy-4-nitrophenyl)-3-(4-nitrophenyl)-5-(2,4-disulfophenyl)-2H-tetrazolium, monosodium salt in the WST-8 assay forms soluble formazan product after interacting with viable cells. Consequently, no additional dissolution procedure,

which might result in sample loss, is required to dissolve the formazan, making WST-8 assay a more sensitive cell viability assay. Similar to the trend depicted in Figure 2, decreasing A549 cell viability with increasing concentration of F-G exposure was noted in Figure 3 for all three nanomaterials examined, and again F-G596 showed the steepest drop in cell viability, changing from 100% at the lowest concentration to 6.8% at the highest concentration. In addition, likewise to the MTT assay data, the cytotoxicity of the three F-G is in the order of F-G596 > F-G597 > F-G595. In both assays, the least toxic F-G595 induced very low cytotoxicity to A549 cells, as the loss in cell viability was only 23.2% (MTT assay) and 13.0% (WST-8 assay) at a very high dosage of 400 μg mL^{-1} F-G exposure.

Since the toxicity profile trends of the F-G acquired from the MTT assay and WST-8 assay were coherent and consistent, we moved on to look into the factors that attributed to the differences in the degree of cytotoxicity induced by the three F-G. Judging from the elemental composition of the three F-G (Table 1), even though we believed that the amount of fluorine found in the nanomaterial plays a role in affecting the F-G's cytotoxicity, it might be harsh to simply conclude that an increase in fluorine content in the F-G will contribute to higher cytotoxicity of the nanomaterial as F-G597 which has the highest at% of F available (50.7 at%) is at least 3 times less toxic than F-G596, which contains 42.6 at% of F. In-depth analysis of the types of carbon-fluorine bonding found in the F-G (Figure 1), however, might shed some light on the toxicity profile trends observed in this study. Between F-G596 and F-G597, although both contain large quantity of fluorine atoms, the amount of individual carbon-fluorine bonds in the two nanomaterials were largely different; the carbon atoms in F-G596 were mainly mono-substituted with fluorine while F-G597 has more carbon atoms which were di-substituted/tri-substituted with fluorine. This contrast could possibly be the determining factor on their cytotoxicity profile as it had been reported in the past that lower level of toxicological effect in fluoro-substituted alkanes / alkenes was associated with increasing number of fluorine atoms in the molecule.[22] In addition, there is also a likelihood that F-G595 exhibited low cytotoxicity as a result of being less exfoliated than the other two fluorinated graphene. This positive correlation between the level of exfoliation of a material and its cytotoxicity has been observed in other 2D nanomaterials such as MoS_2[37].

Besides that, it had been demonstrated in a previous study that the intermediate product, HO-GO, induced a dose-dependent toxicity on A549 cells, with approximately 43% (from MTT assay) and 50% (from WST-8 assay) of the cells remaining viable after incubating the cells with 400 μg mL^{-1} of HO-GO for 24 hours.[38] By comparing the cytotoxicity profiles between HO-GO and the three F-G, we inferred that the fluorination procedure have altered the cytotoxicity of the final products, either by making them less toxic (in the case of F-G595 and F-G597) or more toxic (in the case of F-G596). Consequently, it was believed that the absolute amounts of fluorine found in the nanomaterial, as well as the extent of fluoro-substitution are likely to be the critical factors influencing the trends observed.

F-G nanomaterials-induced interference on cell viability assays

It is well-known that particles in the nanometre scale range might cause the absorbance measurements of cell viability assays such as MTT, WST-1 and XTT to be erroneous, leading to false estimation of the nanomaterials' cytotoxicity.[39-41] Interference on the absorbance readouts could be the result of 1) light scattering / absorbance by the nanomaterials present in the assay during measurement, 2) reduction of the viability markers by the nanomaterials in the absence of viable cells, or 3) removal of insoluble formazan product that are bound to the nanomaterials prior to the absorbance measurements.[40] For example, nanoparticles such as titanium dioxide and zinc oxide which are capable of absorbing and scattering light in the UV and visible light region may affect the cell viability data obtained if they are found in significant quantities in the assay during the absorbance measurements.[42] Studies involving carbon-based nanomaterials like carbon black, carbon nanotubes and graphene had demonstrated that these nanomaterials either react with MTT viability markers or bind to the insoluble purple MTT formazan, thus altering the absorbance value derived subsequently.[39,43-46] In view of the likelihood of F-G nanomaterials inducing similar artifacts on the MTT assay, we performed two assessments to determine whether there are significant interactions between the F-G nanomaterials and the MTT assays in the absence of cells.

Different concentrations of F-G were mixed with the MTT reagent under cell-free conditions and incubated at 37 °C for 3 h in the first assessment to determine if the MTT viability markers will be reduced by F-G. Figure 4A shows the normalized percentage of formazan generated and clearly no reduction of the MTT viability markers by F-G took place as the normalized percentages recorded were all ≤100% (71.9% – 100%) across all three F-G. However, it was noted from the figure that there was a gradual decrease in the normalized percentages of all the three F-G, which could probably be the result of scattering effect caused by the nanomaterials during the absorbance measurements. Similar trend was observed in a previous report by our group involving the cytotoxicity study of fluorinated nanocarbons.[25] Since the drop in the normalized percentages were less than 20% (except at the highest concentration of 400 μg mL^{-1} F-G) and substantial washings were carried out to remove most of the F-G before incubating

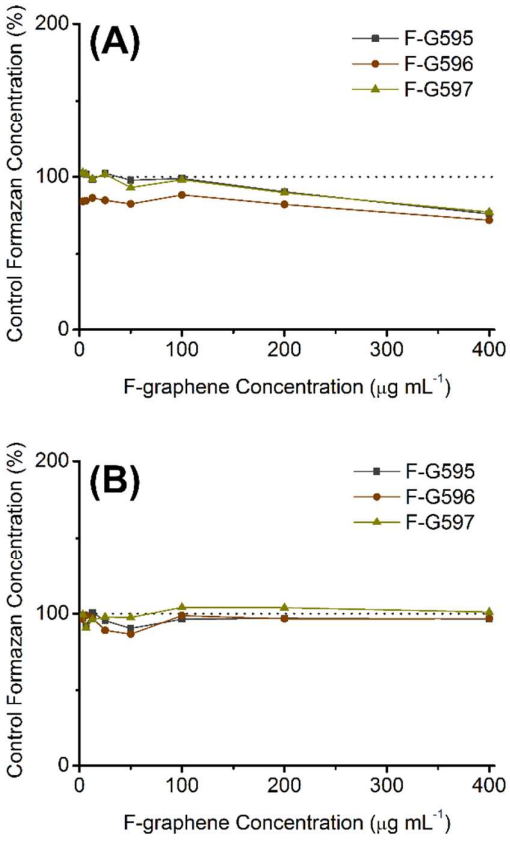

Figure 4. Normalized percentage of formazan generated from the incubation of fluorinated graphene (F-G) in MTT assay under cell-free conditions, showing (A) the extent of MTT viability markers' reaction with different concentrations of F-G and (B) the binding magnitude between MTT/formazan product and the F-G. Black dash lines in both (A) and (B) represent the absorbance of the blank control.

the F-G exposed-cells with the MTT assay during the cytotoxicity examination experiments, this scattering interference by the F-G nanomaterials on the MTT assay was considered insignificant and would not render our MTT cell viability data invalid.

The second assessment was conducted to examine if the insoluble MTT formazan product will bind to the F-G nanomaterials and be removed subsequently during centrifugation. By subjecting ascorbic acid to the cell-free, pre-incubated (3 h) MTT-F-G mixtures for an hour of incubation at 37 °C, the MTT reagent will be reduced into the formazan product.[47] The mixtures were then centrifuged before performing absorbance measurements and the normalized percentages of formazan formed are shown in Figure 4B. The normalized percentages recorded showed only slight variation from 100% (approx. ±10%), thus indicating that there were no interference arising from binding between the F-G nanomaterials and the MTT formazan product, and the MTT cell viability results in Figure 2 can be deemed as interference-free.

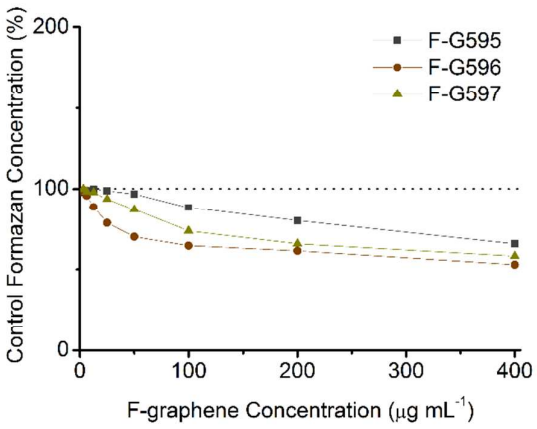

Figure 5. Normalized percentage of formazan generated from the incubation of fluorinated graphene (F-G) in WST-8 assay under cell-free conditions, showing the extent of WST-8 viability markers' reaction with different concentrations of F-G. Black dash line in the graph represents the absorbance of the blank control.

WST-8 assay has also been shown to be able to react with nanomaterials without the presence of viable cells to produce soluble formazan product.[48,49] Therefore, we investigated the possibility of WST-8 formazan generation by F-G in the absence of viable cells. The relative percentages of the WST-8 formazan produced, calculated from the absorbance readings of the mixtures containing WST-8 assay and varying concentrations of F-G, are illustrated in Figure 5. Similar to the data obtained in Figure 4A, no reduction of WST-8 viability markers were detected across all three F-G. Instead, they experienced gradual decrease in the normalized percentages with increasing amounts of F-G, indicating that the light scattering effect induced by these nanomaterials disrupts the WST-8 absorbance measurements as well. Although the drop in the normalized percentages from the WST-8 measurements (52.9% – 100%) is relatively higher as compared to the values from the MTT measurements, we believe that the credibility of the WST-8 assay data in Figure 3 will be maintained as the absolute drop in the absorbance values only constituted to a marginal decrease in the absorbance readouts from the WST-8 cell viability experiments.

Conclusions

In this study, we investigated the cytotoxicity of three F-G nanomaterials with differing elemental content. These F-G nanomaterials have the potential to be applied commercially and thus it was necessary to determine whether they are hazardous to mammalian cells. Based on the cell viability assessments results, it seemed that F-G with higher amounts of fluorine atoms, especially those rich in monofluoro-substituted groups, imparted higher toxicological effects on A549 cells. However, it might be beneficial to screen more F-G nanomaterials before a more conclusive statement is made. Nonetheless, manufacturers who are producing these nanomaterials should indicate clearly the elemental

composition and types of fluorine-containing groups present in the future. Lastly, the three F-G nanomaterials were examined for possible particle-induced interference on the cell viability assays (MTT and WST-8 assays), and absorbance data acquired from the experiments suggested that the F-G did not interact with both MTT and WST-8 assays significantly to create any distortion in the cell viability values.

Acknowledgements

M.P. was supported by Tier 2 grant from Ministry of Education, Singapore. Z.S., F.Š. and Z.J. were supported by Czech Science Foundation (GACR No. 15-09001S).

References

1 L. Tian, D. Ghosh, W. Chen, S. Pradhan, X. Chang and S. Chen, *Chem. Mater.*, 2009, **21,** 2803-2809.
2 M. Zhang and M. Yudasaka, *Carbon*, 2014, **69,** 642.
3 D. S. Su, S. Perathoner and G. Centi, *Chem. Rev.*, 2013, **113,** 5782-5816.
4 Project on emerging nanotechnologies (PEN). On-line inventory of nanotechnology-based consumer products. Accessed 13th March 2015. Available at: www.nanotechproject.org/cpi/about/analysis/, 2015
5 K. S. Novoselov, V. I. Falko, L. Colombo, P. R. Gellert, M. G. Schwab and K. Kim, *Nature*, 2012, **490,** 192–200.
6 A. K. Geim and K. S. Novoselov, *Nat. Mater.,* 2007, **6,** 183–191.
7 A. K. Geim, *Science,* 2009, **324,** 1530–1534.
8 J. E. Johns and M. C. Hersam, *Acc. Chem. Res.,* 2012, **46,** 77–86.
9 a) A. Ambrosi, A. Bonanni, Z. Sofer, J. S. Cross and M. Pumera, *Chem.–Eur. J.,* **2011,** 17, 10763–10770. b) E. L. K. Chng, M. Pumera, *RSC Adv.* 2015, **5**, 3074. c) M. Pumera, *Chem Asian J.* 2011, **6**, 340.
10 F. Karlický, K. K. R. Datta, M. Otyepka and R. Zbořil, *ACS Nano,* 2013, **7,** 6434–6464.
11 Jeon, K. J.; Lee, Z.; Pollak, E.; Moreschini, L.; Bostwick, A.; Park, C. M.; Mendelsberg, R.; Radmilovic, V.; Kostecki, R.; Richardson, T. J.; Rotenberg E., *ACS Nano,* 2011, **5,** 1042–1046.
12 Q. Feng, Q. Cao, M. Li, F. Liu, N. Tang and Y. Du, *Appl. Phys. Lett.,* 2013, **102,** 013111.
13 Z. Wang, J. Wang, Z. Li, P. Gong, X. Liu, L. Zhang, J. Ren, H. Wang and S. Yang, *Carbon,* 2012, **50,** 5403-5410.
14 R. R. Nair, W. Ren, R. Jalil, I. Riaz, V. G. Kravets, L. Britnell, P. Blake, F. Schedin, A. S. Mayorov, S. Yuan, M. I. Katsnelson, H.-M. Cheng, W. Strupinski, L. G. Bulusheva, A. V. Okotrub, I. V. Grigorieva, A. N. Grigorenko, K. S. Novoselov and A. K. Geim, *Small*, 2010, **6,** 2877-2884,
15 P. Gong, Z. Wang, J. Wang, H. Wang, Z. Li, Z. Fan, Y. Xu, X. Han and S. Yang, *J. Mater. Chem.,* 2012, **22,** 16950-16956.
16 Y. Wang, W. C. Lee, K. K. Manga, P. K. Ang, J. Lu, Y. P. Liu, C. T. Lim, K. P. Loh, *Adv. Mater.,* 2012, **24,** 4285-4290.
17 H.-G. Oh, H.-G. Nam, D.-H. Kim, M.-H. Kim, K.-H. Jhee and K. S. Song, *Mater. Lett.,* 2014, **131,** 328-331.
18 T. Okazoe, *Proc. Jpn. Acad. Ser. B*, 2009, **85,** 276-289.
19 Banks RE, Tatlow JC. in Fluorine: The First Hundred Years (1886-1986). Banks RE, Sharp DWA, Tatlow JC (Eds). Elsevier Science Publishing Co., Inc., NY, USA, 93-97 (1986).
20 A. Proudfoot, S. Bradberry and J. A. Vale, *Toxicol Rev*, 2006, **25,** 213-219.
21 N. V. Goncharov, R. O. Jenkins and A. S. Radilov, *J. Appl. Toxicol.*, 2006, **26,** 148-161.
22 J. W. Clayton, Jr., in *Pharmacology of fluorides*, ed. F. Smith, Springer Berlin Heidelberg, 1966, vol. 20, ch. 9, pp. 459-500.
23 R. Romero-Aburto, T. N. Narayanan, Y. Nagaoka, T. Hasumura, T. M. Mitcham, T. Fukuda, P. J. Cox, R. R. Bouchard, T. Maekawa, D. S. Kumar, S. V. Torti, S. A. Mani and P. M. Ajayan, *Adv. Mater.,* 2013, **25,** 5632-5637.
24 O. Barbier, L. Arreola-Mendoza and L. M. Del Razo, *Chem. Biol. Interact.*, 2010, **188,** 319-333.
25 W. Z. Teo, C. K. Chua, Z. Sofer, and M. Pumera, *Chem.–Eur. J.,* 2015, **21,** 13020-13026.
26 T. Mosmann, *J. Immunol. Methods*, 1983, **65,** 55-63.
27 M. Ishiyama, Y. Miyazono, M. Shiga, K. Sasamoto, US Pat., 6,063,587, 2000.
28 U. Hofmann and A. Frenzel, *Kolloid Z.*, 1934, **68,** 149-151.
29 C. H. A. Wong, O. Jankovský, Z. Sofer and M. Pumera, *Carbon*, 2014, **77,** 508-517.
30 S. Rozen, in *Efficient Preparations of Fluorine Compounds*, John Wiley & Sons, Inc., 2012, DOI: 10.1002/9781118409466.ch25, pp. 146-153.
31 A. Bianco, *Angew. Chem., Int. Ed.*, 2013, **52,** 4986-4997.
32 D. Richards and A. Ivanisevic, *Chem. Soc. Rev.*, 2012, **41,** 2052-2060.
33 J. T. Robinsons, J. S. Burgess, C. E. Junkermeier, S. C. Badescu, T. L. Reinecke, F. K. Perkins, M. K. Zalalutdniov, J. W. Baldin, J. C. Culbertson, P. E. Sheehan and E. S. Snow, *Nano Lett.,* 2010, **10,** 3001-3005.
34 Z. Wang, J. Wang, Z. Li, P. Gong, X. Liu, L. Zhang, J. Ren, H. Wang and S. Yang, *Carbon,* 2012, **50,** 5403-5410.
35 D. K. Samarakoon and X-Q. Wang, *ACS Nano,* 2009, **3,** 4017-4022.
36 D. K. Samarakoon, Z. Chen, C. Nicolas and X-Q. Wang, *Small,* 2011, **7,** 965-969.
37 E. L. K. Chng, Z. Sofer and M. Pumera, *Nanoscale,* 2014, **6,** 14412-14418.
38 E. L. K. Chng, Z. Sofer and M. Pumera, *Chem. –Eur. J.,* 2014, **20**, 6366-6373.
39 N. A. Monteiro-Riviere, A. O. Inman and L. W. Zhang, *Toxicol. Appl. Pharmacol.*, 2009, **234,** 222-235.
40 A. L. Holder, R. Goth-Goldstein, D. Lucas and C. P. Koshland, *Chem. Res. Toxicol.*, 2012, **25,** 1885-1892.
41 A. Casey, E. Herzog, M. Davoren, F. M. Lyng, H. J. Byrne and G. Chambers, *Carbon*, 2007, **45,** 1425-1432.
42 A. Kroll, M. Pillukat, D. Hahn and J. Schnekenburger, *Arch Toxicol*, 2012, **86,** 1123-1136.
43 K.-H. Liao, Y.-S. Lin, C. W. Macosko and C. L. Haynes, *ACS Appl. Mater. Interfaces*, 2011, **3,** 2607-2615.
44 N. A. Monteiro-Riviere and A. O. Inman, *Carbon*, 2006, **44,** 1070-1078.
45 L. Belyanskaya, P. Manser, P. Spohn, A. Bruinink and P. Wick, *Carbon*, 2007, **45,** 2643-2648.
46 J. M. Wörle-Knirsch, K. Pulskamp and H. F. Krug, *Nano Lett.*, 2006, **6,** 1261-1268.
47 R. Chakrabarti, S. Kundu, S. Kumar and R. Chakrabarti, *J. Cell. Biochem.*, 2001, **80,** 133-138.
48 N. M. Latiff, W. Z. Teo, Z. Sofer, Š. Huber, A. C. Fisher and M. Pumera, *RSC Adv.*, 2015, **5,** 67485-67492.
49 N. M. Latiff, W. Z. Teo, Z. Sofer, A. C. Fisher and M. Pumera, *Chem.–Eur. J.*, 2015, **21,** 13991-13995.

